Phase behavior and chain dynamics of elastin-like peptides versus amino acid sequences

Jany Dandurand[1] · Valérie Samouillan[1] · Colette Lacabanne[1] · Antonietta Pepe[2] · Brigida Bochicchio[2]

Abstract Elastin fibrillogenesis is conditioned by multiple self-assembly processes. Previous studies have evidenced the crucial influence of amino acid specificities on molecular organization of glycine-rich elastin-like peptides, but also the important role of environment on the self-assembly processes. For the first time, we combined a differential scanning calorimetry (DSC) study on aqueous solutions of three elastin-like peptides with thermally stimulated currents (TSC) experiments in the condensed state. We have studied three pentadecapeptides having the XGGZG motif threefold repeated with *X* and *Z* residues constituted of valine and leucine, known to form fiber structures. Valine and leucine moieties differ only by the presence of $–CH_2–$ spacer occupying in the pattern the first or the fourth position. Both of the residues are among the most abundant in elastin. Via DSC, we showed that the simple substitution of one amino acid strongly influences the surrounding hydration of the pentadecapeptides. During the self-assembly process, a slow exchange between bound water and bulk water is highlighted for $(VGGLG)_3$, whereas a fast exchange of water molecules is found for $(VGGVG)_3$ and $(LGGVG)_3$. In the pre-fibrillar condensed state, TSC analysis reveals localized and delocalized motions and gives a fingerprint of the dynamics via activation parameters. At the localized level, a profound difference in the carbonyl environment is observed between $(VGGLG)_3$ and the other peptides. The delocalized chain dynamics of the three peptides can be connected to the different conformations. The dominant unordered conformation of $(VGGLG)_3$ leads to a softer system, while the large amount of β sheets and β turns in $(VGGVG)_3$ and $(LGGVG)_3$ leads to stiffer systems. Around the physiological temperature occurs a structural, isochronal phase transition, sequence specific, suggested to be associated with the ferroelectricity of such elastin-like peptides.

Keywords Elastin-like peptides · LCST transition · Self-assembly · Molecular mobility · Structural transition

✉ Jany Dandurand
jany.lods@univ-tlse3.fr

[1] CIRIMAT, Physique des Polymères, Université de Toulouse, Université Paul Sabatier, 31062 Toulouse, France

[2] Dipartimento di Scienze, Universita degli Studi della Basilicata, via dell'Ateneo Lucano, 10, 85100 Potenza, Italy

Introduction

Elastin-like peptides (ELPs) rich in proline residues such as $(VPGXG)_n$ and $(GXGVP)_n$ are widely studied as consistent models [1–3] of tropoelastin hydrophobic domains. These ELPs show a phase transition in response to temperature increase [2, 4], at a characteristic value of temperature called lower critical solution temperature (T_t or LCST) as well described by Urry [5] and Kurzbach [6]. The reversible transition temperature T_t of ELPs depends on the solution concentration and composition: in a peculiar range of concentration, this transition reaches a constant value also called the lower critical solution temperature (LCST). The LCST also depends on the chain length [7] and on the moieties nature [8]. This transition is interpreted in terms of hydrophobic effects [9]. In aqueous solution, below T_t the free polymer chains are disordered, random coiled and fully hydrated. In this random coil conformation of the polypeptide chains, apolar residues are exposed to water molecules that organize in a clathrate-like form, more structured than bulk water. This hydration is known as the oxymoron "hydrophobic hydration" [5, 10]. Above *Tt,* the

chains fold triggered by hydrophobic driving force and self-assemble resulting in a phase separation. In diluted solutions of poly(GVGVP), the two resultant phases of the coacervate are equilibrium water and a structured phase constituted by 63% of water and 37% of polypeptide by mass [5].

Bochicchio et al. [11] evidenced the importance of proline residues in the reversible temperature-induced coacervation process, the proline-rich ELPs having a strong propensity to coacervate. This constitutes a critical and preliminary step for the self-assembly of tropoelastin in vivo, through dehydration and rehydration of hydrophobic side chains. Contrarily, glycine-rich domains show an irreversible temperature transition, dependent on dehydration and conformation, giving rise to aggregates similar to amyloid-like fibers [12–15]. These self-assembled states induce a small increase in viscosity [16]. Miao et al. [17] investigated the specific role of domain sequence and organization on the tensile mechanical properties of cross-linked ELP. Furthermore, Muiznieks [18] compared the contributions of proline-poor hydrophobic sequences to self-assembly and to the tensile properties through the characterization of phase transition. These works allowed the development of a novel class of double hydrophobic block polypeptides—alternating proline-rich and glycine-rich sequences—for tissue engineering [19]. Representative examples of glycine-rich sequences are $(LGGVG)_7$ and $(VGGVG)_5$. These sequences were characterized by circular dichroism, FTIR, XPS and AFM [20] in different conditions [21]. Poly(VGGVG), obtained by polycondensation reaction, adopts in water an amyloid-like structure characterized by β sheet-rich conformations [22]. Moscarelli et al. [23] compared secondary structures and supramolecular organization of (VGGVG), poly(VGGGV) and $(VGGVG)_3$ and demonstrated that $(VGGVG)_3$ self-assembles. NMR in aqueous solution showed that β-strands coexist with random coil conformation [24] in $(VGGVG)_3$ peptide while solid state FTIR studies evidence that the post-aggregated peptide adopts a β-sheet conformation. At the supramolecular level, AFM in different environments assessed the existence of fibrils in $(VGGVG)_3$ after 1 h of incubation at 37 °C, increasing in size with time.

The aim of this work was to characterize the repetitive glycine-rich peptides $(XGGZG)_3$ (X, $Z = V$ or L) by thermal and dielectric analysis in a systematic approach to understand the physical origin of LCST as well as the modifications of the molecular conformation and hydration states. These pentadecapeptides provide the peculiar and unique properties of tropoelastin, due to the presence of hydrophobic residues, and are also able to form amyloid-like fibrils [22, 24]. That finding represents an additional value in the tissue engineering field.

Differential scanning calorimetry has proved to be an useful technique to study phase transitions in proteins mixtures [25], protein denaturation in biological compounds [26], aggregation and self-assembly of proteins and peptides [27, 28] and for analyzing recurring sequences of elastin such as pentapeptide GLGGV [29], poly(GVGVP) [30]. Finally, it also runs in solution, evidencing for example the hydrophobic hydration of poly(VPGVG) [9] and the water structure in elastin-like peptides [31].

Dielectric techniques are well suited to investigate the dynamics of proteins through the scan over a wide range of frequency/lengths [32]. TSC experiment is a powerful technique to scan the chain dynamics of native elastin both in the freeze-dried and hydrated states [33–35] as well as short elastin-derived peptides and polypeptides [29, 36, 37] in the nanometric range. This high-resolution technique is peculiarly adapted to scan the amorphous phase in biopolymers and peptides far from their degradation, often few resolved with classical techniques [38].

The combination of thermal and dielectric techniques is innovative to obtain fine information from both states (diluted and condensed) of the three pentadecapeptides. The influence of moieties position in the peptides chain on the mechanism of aggregation, phase separation and molecular mobility can be evaluated trough thermal and dielectric data.

Materials and methods

Peptide synthesis, disaggregation and purification

The peptides were synthesized by SPPS on the Tribute automatic peptide synthesizer (Protein Technologies Inc, Arizona, USA) by using a standard 9-fluorenylmethoxycarbonyl (Fmoc) protection peptide synthesis protocol. The cleavage of peptide from the resin was achieved by using an aqueous mixture of 95% trifluoroacetic acid (TFA). The peptides were lyophilized. Three milligrams of lyophilized peptides was dissolved in 1 cm^{-3} of TFA and gently stirred at 373 K for 3 h to completely dissolve the seeds responsible for the insolubility of peptide (unseeded peptide). Upon addition of 9 cm^{-3} of ultrapure water, the solution was fractionated into equal parts and lyophilized. This procedure provided a powder aliquot for HPLC. The peptides were purified by semi-preparative reversed-phase high-performance chromatography on a Shimadzu automated HPLC system supplied with a semi-preparative Jupiter C18 column (Phenomenex, 250. 10 mm, 5 μm). A binary gradient was used, and the solvents were H_2O (0.1% TFA) and CH_3CN. The purity of peptides was assessed by ESI (electrospray), Fourier transform mass (FTMS) and ^{1}H-NMR spectroscopy.

Differential scanning calorimetry

The differential scanning calorimetry (DSC) curves were recorded with a Pyris Diamond calorimeter (Perkin Elmer, USA). The calorimeter was calibrated using cyclohexan and indium as standards. Solution samples (15 μL) were sealed in hermetic aluminum pans, and an empty pan was used as reference. Cooling and heating rates were chosen to obtain well-defined and reproducible results, usually at 10 °C min^{-1}. The concentration of polypeptides was 10^{-3} g cm^{-3} in ultrapure water or in solution buffer in order to compare the results with turbidimetry assays. Two distinct DSC protocols (Fig. 1) were applied, including successive heating/cooling scans, with or without an isotherm at 37 °C for 1 h. The final temperature of the successive scans increases step by step until 80 °C.

Thermostimulated currents

Complex TSC curves

Complex thermostimulated currents (TSC) experiments were carried out using a TSC/RMA Analyzer (SETARAM Instrumentation, Caluire, France). Freeze-dried powder samples, 1 mg in mass, were placed between two stainless steel electrodes surrounded by a Teflon ring. The sample thickness is 140 μm. Before experiments, the cryostat was flushed and filled with dry helium to ensure good thermal exchange. For complex experiments, the sample was polarized by a static electric field $E = 4000$ V mm^{-1} over a temperature range from the poling temperature ($T_p = -20$ °C and $T_p = 110$ °C) down to the freezing temperature $T_0 = -150$ °C with a fast cooling. Then, the field was turned off and the depolarization current was recorded with a controlled heating rate ($q = +7$ °C min^{-1}); the equivalent frequency of the TSC curve was feq $\sim 10^{-2}$–10^{-3} Hz. These experimental conditions chosen to optimize the resolution are classically used for synthetic and biological systems [32, 38].

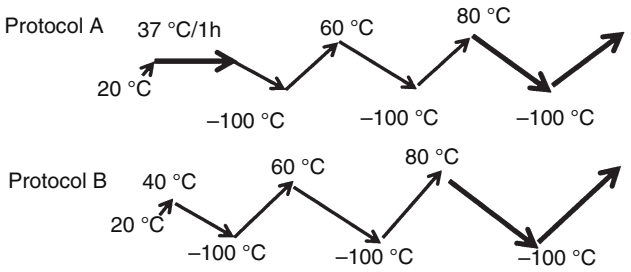

Fig. 1 DSC experimental protocols

Elementary TSC curves

Elementary TSC curves were obtained by using fractional polarizations (TSC/FP) with a polarization window of 5 °C. The field was removed and the sample cooled to a temperature $T_0 = T_p - 40$ °C. The depolarization current was recorded with a constant heating rate $q = +7$ °C min^{-1}. The series of elementary curves was generated by shifting the polarization window by 5 °C between 60 and 110 °C.

Results and discussion

Thermal response of $(VGGVG)_3$

The first step of the experiment performed in the calorimeter is an incubation protocol according to the works of Moscarelli [23] and Bochicchio [8]. After 1 h at 37 °C, according to previous studies, fibrils are obtained [8, 23]. The corresponding isotherm recorded by DSC with $(VGGVG)_3$ is plotted in Fig. 2.

At 37 °C, the isotherm curve exhibits an endothermic event occurring at 1.5 min and attributed to the lower critical solution temperature/LCST transition [1, 5]. It must be recalled that hydrophobic groups of the peptides are initially surrounded by ordered pentagonal rings water [39]. The disordering of hydrophobic hydration is the driving process of the inverse temperature transition phenomenon. At the transition, the two-component system constituted of $(VGGVG)_3$ and water becomes more disordered. It may also be noted that the van der Waals interactions due to associations between hydrophobic groups as the transition goes forward are exothermic, but necessarily

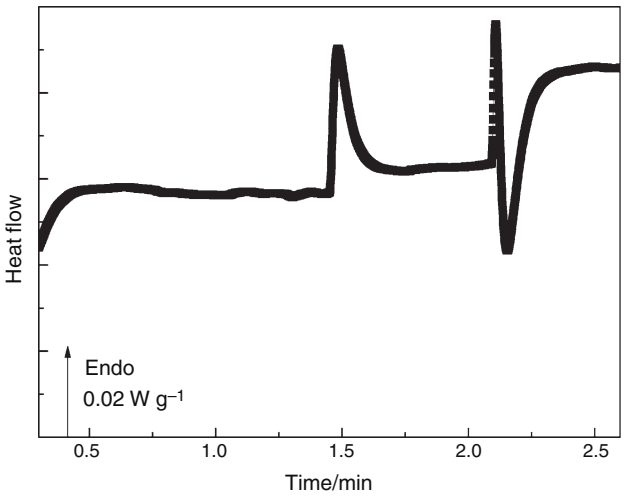

Fig. 2 Isotherm DSC response recorded for $(VGGVG)_3$ in pure water (10^{-3} g cm^{-3}) at 37 °C

of lesser magnitude; otherwise, the inverse temperature transition would not be an endothermic transition.

An endo-/exothermic mechanism associated with a crystallization or a nucleation–polymerization process, similar to aggregation [40, 41], is noted at around 2.1 min. After the twin thermic responses, $(VGGVG)_3$ was aggregated in fibrils of variable width and length [42]. According to Cirulis and Keeley, above the LCST occurs a second temperature-dependent transition characterized by a change of viscosity, strong shear thinning and high ratio of storage to loss moduli. This state is reversible if the temperature is immediately lowered. An incubation time above this temperature limits this thermal reversibility [16].

After this isothermal step, four heating and cooling runs were recorded (Fig. 1 protocol A). The successive cooling and heating scans were applied for the $(VGGVG)_3$ solution in pure water, resulting in the DSC curves reported in Fig. 3.

On the heating curves, an endothermic peak is observed at around 0 °C and associated with the melting temperature of primary ice; an exothermic peak is present on the cooling curves in the [−20; −10 °C] zone. This exothermic peak is ascribed to the crystallization of water and shifts toward high temperature with the successive temperature scans performed until 80 °C (see insert of Fig. 3).

In parallel was applied the protocol B constituted by successive scans (heating/cooling) without the preliminary incubation step at 37 °C. In this case, four consecutive curves of $(VGGVG)_3$ peptide in pure water (10^{-3} g cm^{-3}) were recorded. In Fig. 4, only the cooling curves are reported for the sake of clarity.

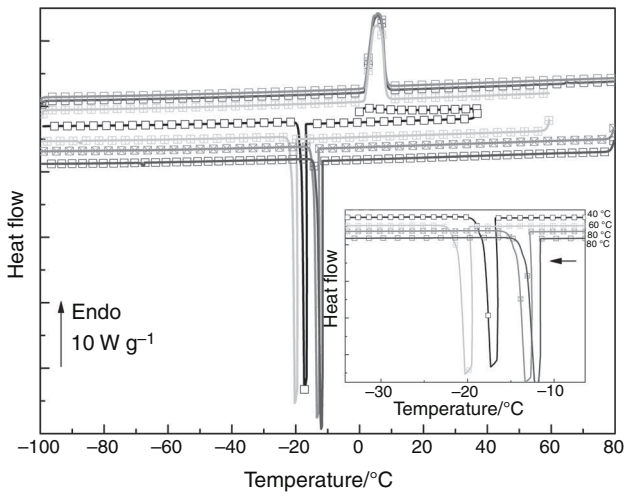

Fig. 3 DSC curves of $(VGGVG)_3$ in pure water (10^{-3} g cm^{-3}) obtained with protocol A (temperatures noted in the *right side* indicated the final temperature of the heating ramp performed just before the cooling ramp). The length of the *vertical arrow* corresponds to the scale

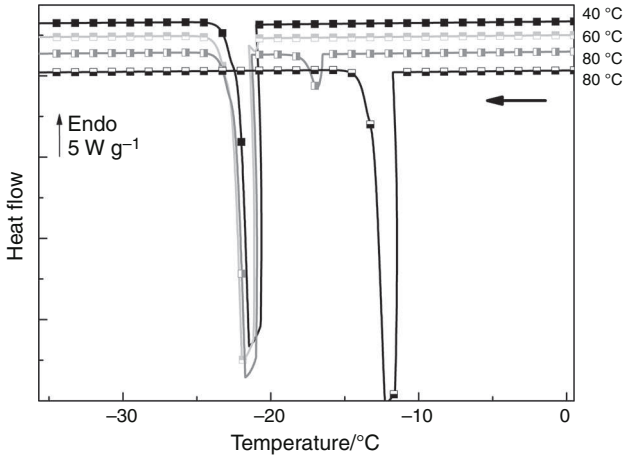

Fig. 4 DSC curves of $(VGGVG)_3$ in pure water (10^{-3} g cm^{-3}) obtained with protocol B (temperatures noted in the *right side* indicate the final temperature of the heating ramp performed just before the cooling ramp). The length of the *vertical arrow* corresponds to the scale

On the cooling curves, we can observe a drastic change in the crystallization phenomenon when the pentadecapeptide solution was preliminary heated until 80 °C. The initial exothermic transition recorded at −20 °C, namely the freezing of bound water [43, 44], evolves step by step. A second contribution, visible as a shoulder (see arrow in Fig. 4), appears with the increase in the temperature until 60 °C. On the successive cooling scan, two exothermic peaks take place: At low temperature, an important contribution of the freezing bound water occurs, while at higher temperature a weak contribution of the freezing bulk water emerges. Finally, after the completion of two heating scans until 80 °C a single transition is evidenced at −13 °C, namely the freezing bulk water. This indicates that the disordering of hydrophobic hydration is achieved.

The influence of the thermal history on the water crystallization of the $(VGGVG)_3$ system is illustrated in Fig. 5.

With the preliminary incubation step (37 °C for 1 h), the crystallization of bulk water at −17 °C is associated with the achievement of the phase separation process. Without this incubation step, a preliminary heating at 80 °C allows to detect the freezing of bound water at −22 °C and the weak contribution of bulk water [43] at −17 °C, testifying the outset of the phase separation process. It is noteworthy that the total crystallization enthalpy is constant in both the cases, attesting of the transfer process.

In brief, the progressive expulsion of water from the first hydration layer toward bulk water, mimicking the fibril formation, can be can be tracked through the water crystallization behavior.

Previous turbidimetry studies [8] demonstrated that $(VGGVG)_3$ incubated at 37 °C is able to self-aggregate after 1 week in water and after only 1 day if incubated in

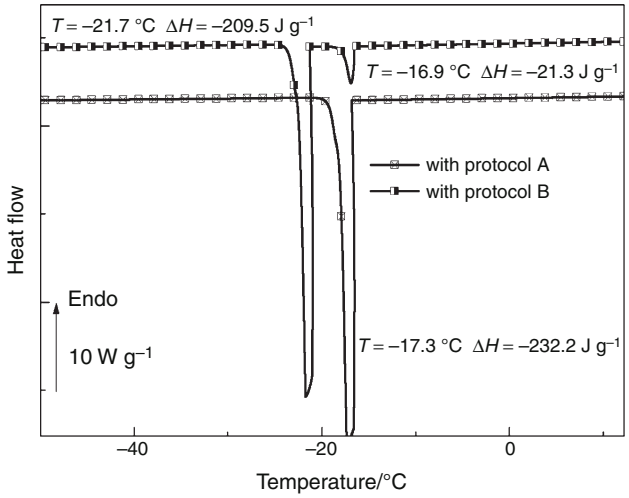

Fig. 5 Comparison of the DSC cooling curves of $(VGGVG)_3$ in pure water (10^{-3} g cm^{-3}) from protocols A and B after a first heating until 80 °C. The length of the *vertical arrow* corresponds to the scale

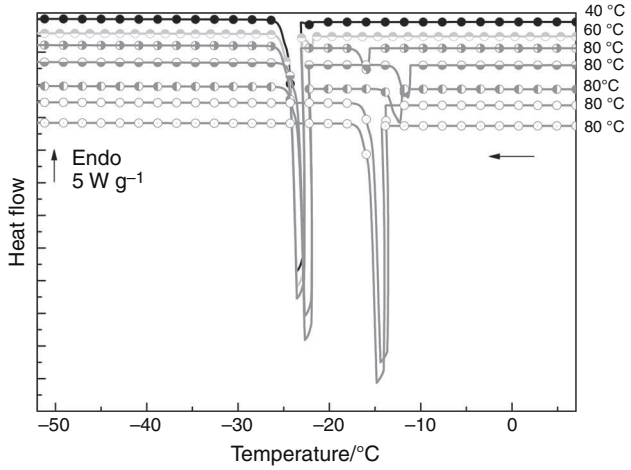

Fig. 6 DSC curves of $(VGGLG)_3$ in pure water (10^{-3} g cm^{-3}) obtained with protocol B (temperatures noted in the *right side* indicated the final temperature of the heating ramp performed just before the cooling ramp). The length of the *vertical arrow* corresponds to the scale

buffer solution. It was also shown that all the peptides are able to self-aggregate. However, the turbidimetric measurements provide poor information on the structure and almost none about the role played by the solvation [8]. Therefore, calorimetry measurements were performed on $(VGGLG)_3$ and $(LGGVG)_3$ in order to gain complementary information. The same incubation conditions as turbidimetry were used for the DSC study on $(VGGVG)_3$ through successive scans. As a result, some insights were obtained on the effect of the substitution of *V* for *L* in first and fourth positions of (XGGZG) motif.

Thermal response of $(VGGLG)_3$

$(VGGLG)_3$ differs from $(VGGVG)_3$ by the substitution of the fourth moiety, namely by the presence of an additional methylene unit in leucine at the molecular level.

In Fig. 6 are superimposed the DSC curves of $(VGGLG)_3$ obtained with protocol B.

The freezing bound water was visible as a dominant exothermic peak at around −22 °C on the first cooling. This initial exothermic transition evolves step by step until the total transfer of freezing bound to freezing bulk water. This transfer was completely achieved after four heating scans until 80 °C, suggesting a more progressive hydration change for $(VGGLG)_3$ than for $(VGGVG)_3$.

From a conformational point of view, in aqueous solution Bochicchio et al. [8] evidenced for this peptide extended and flexible conformations, such as PPII and unordered structures, with a weak tendency to form turn structures. Generally, an increase in the amount of water from hydrophobic hydration decreases the solubility [4, 45]. It is widely accepted that effect is caused by the specific ways in which polar and apolar groups are hydrated. For this peptide, the release of water molecules in the hydration layer into bulk was slow, correlated with its low propensity to form fibrils.

Thermal response of $(LGGVG)_3$

DSC successive cooling curves (Fig. 7) demonstrated a specific hydrophobic hydration behavior for $(LGGVG)_3$. A single exothermic transition shifting toward high temperature after one heating until 80 °C was observed. In this case, the transfer of freezing bound water to bulk water associated with the phase separation is a one-step mechanism.

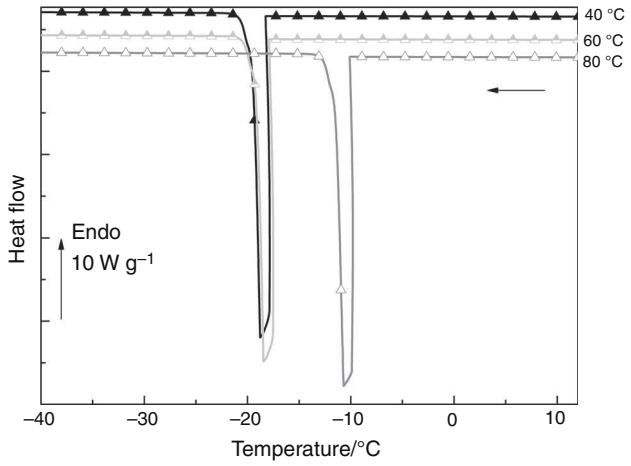

Fig. 7 DSC curves of $(LGGVG)_3$ in pure water (10^{-3} g cm^{-3}) obtained with protocol B (temperatures noted in the *right side* indicated the final temperature of the heating ramp performed just before the cooling ramp). The length of the *vertical arrow* corresponds to the scale

Leucine in the first position of the chain modifies the total hydration behavior of the pentadecapeptide.

Influence of leucine substitution and position

Water environment has a crucial role in fiber formation [24], and we showed that the simple substitution of one amino acid strongly influenced the surrounding hydration of the pentadecapeptides.

Furthermore, molecular dynamic simulations showed that for both $(VGGLG)_3$ and $(LGGVG)_3$ the presence of switched *V/L* leads to strong local conformations of turns [8], and suggested the solvation of peptides is mainly responsible for this finding.

The DSC study highlighted a slow-change water mechanism between bound water and bulk water in $(VGGLG)_3$. The peptide is characterized by the presence of PPII structure at the molecular level and self-aggregated in straight rods at supramolecular level [8]. As for $(VGGVG)_3$ and $(LGGVG)_3$, a fast exchange of water molecules during self-assembly process was found. Even if both of them are characterized by β structures and type II β turns, a phase separation process is observed only for $(VGGVG)_3$ in pure water.

The final heating scan from protocol B evidences at high temperature for the three peptides the ultimate supramolecular organization (Fig. 8).

The endothermic peaks above 50 °C result from the final phase separation, disordering the H-bonded water network and ordering the solid phase of peptides by hydrophobic association. Additionally, each peptide brings has a specific thermal answer. $(LGGVG)_3$ is characterized by two irreversible endothermic peaks at 55 and 70 °C, ascribed to the thermal signature of the high regular organization of the twisted rope fibrils observed in AFM [8].

$(VGGVG)_3$ possesses multiple order–disorder transitions distributed on a broad temperature scale and is characterized by tangled filaments in AFM [8]. Its thermal signature sheds light on the complex structure and length of supramolecular organization described by Moscarelli [23] who noted that $(VGGVG)_3$ formed short amyloid-like fibrils increasing in size with time. In this case, the system can be described by a snowflake model in which fibrils arise from electro-dense nucleation core.

The irreversible and single endothermic peak ascribed to $(VGGLG)_3$ is the thermal signature of the one-step dehydration process, attributed to an ultimate and irreversible transformation of the network. It corresponds to a structural event distinguishable from LCST, according to Cirulis and Keeley [16]. The sequence specificities of this peptide with leucine in fourth position give a characteristic behavior with water environment but also in the time scale of aggregation. This substitution could affect the polarity of the amino acid and the different ways in which polar and apolar moieties are hydrated. As generally described in literature, a decrease in hydrophobic hydration increases the polarity; in this case, the multi-step disorganization of hydrophobic hydration gives rise to a slow increase in polarity.

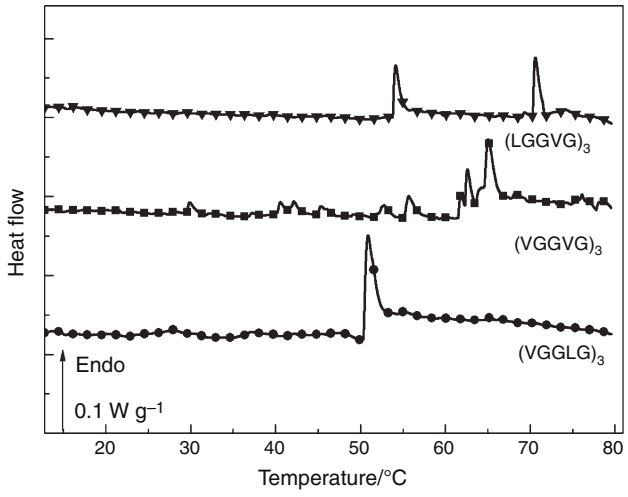

Fig. 8 Final DSC heating scans of pentadecapeptides

Dielectric response

ThermoStimulated Currents have been used to characterize the molecular mobility of pentadecapeptides in the aggregated state over a wide temperature range, giving insights into the pre-fibrillar state. The various peaks appearing in TSC curves characterize the operative molecular mechanism through which an electret stores its charge. In this nonisothermal relaxation, mainly the dipolar species of the polymer are expected to get relaxed.

In Fig. 9, we have reported the low-temperature TSC curves of freeze-dried pentadecapeptides in the initial state and after a heating at 110 °C.

In the pre-fibrillar state, the condensed pentadecapeptides are characterized by a large relaxation mode at around −90 °C, with an intensity ten times higher for $(VGGLG)_3$ than for $(VGGVG)_3$ and five times higher for $(VGGLG)_3$ than for $(LGGVG)_3$. This relaxation labeled β mode in accordance with the literature data is largely evidenced in polypeptides and proteins and assigned to the localized and low cooperative motions of the carbonyl groups/bound water complex [34, 46, 47]. The larger intensity of this mode in $(VGGLG)_3$ could be related to an higher proportion of localized water in this peptide in contrast to $(VGGVG)_3$, which is in good agreement with FTIR results on freeze-dried pre-fibrillar states on these peptides [8]. It

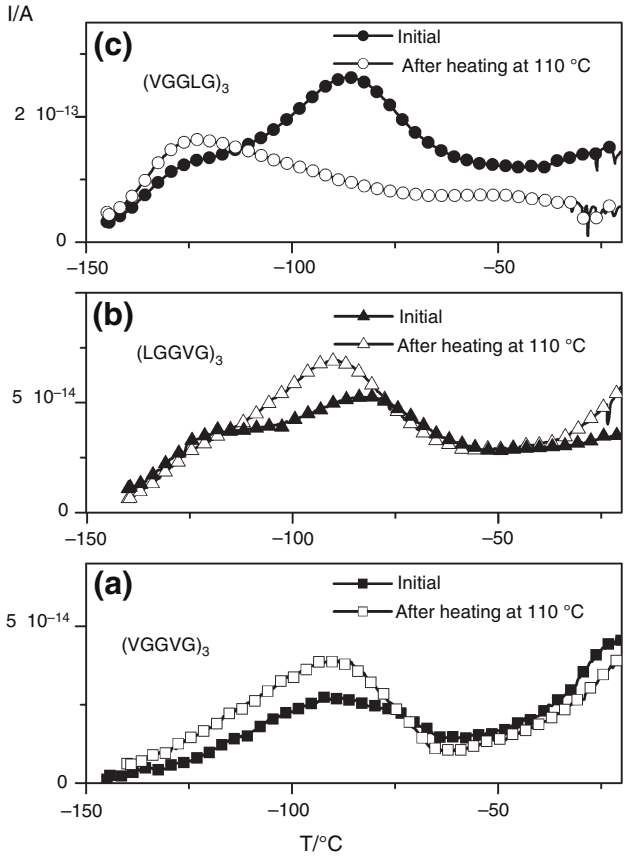

Fig. 9 TSC curves of the freeze-dried pentadecapeptides $(VGGVG)_3$ (**a**), $(LGGVG)_3$ (**b**) and $(VGGLG)_3$ (**c**) obtained after a poling at −20 °C in the initial state and after a heating at 110 °C

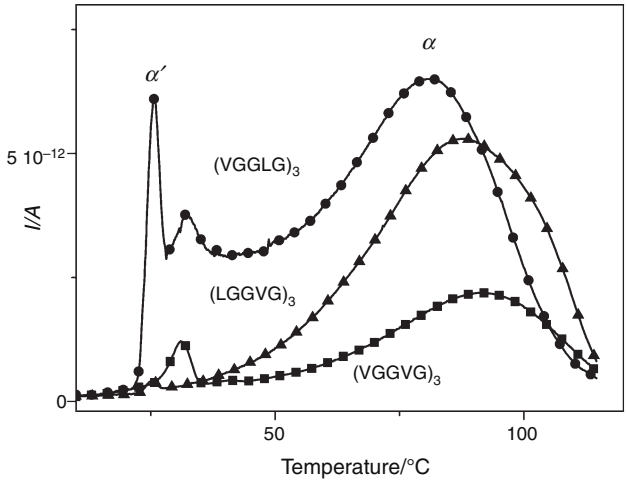

Fig. 10 TSC curves of the pentadecapeptides obtained after a poling at −20 °C in the initial state and after a heating at 110 °C

is also noteworthy that the β mode of $(VGGLG)_3$ completely vanishes with dehydration at 110 °C while it slightly increases after this heating for $(LGGVG)_3$ and $(VGGVG)_3$, attesting to a profound difference in carbonyl environment in this former peptide. It can be suggested that the unordered conformation and the PPII structure evidenced by FTIR [8] in this former peptide allow the storage of an important amount of water in the initial state and the complete dehydration with an heating at 110 °C. In contrast, the dominant β sheets and β turns conformations evidenced in $(LGGVG)_3$ and $(VGGVG)_3$ prevent these peptides from storing important amount of water, and the heating allows in this case a densification of these structures making the local reorientation of the intrinsic carbonyl group more resolved in TSC curves.

In Fig. 10 are reported the high-temperature curves of the freeze-dried peptides.

In the [20; 40 °C] temperature zone are evidenced sharp and intense modes (α'), 5–6 °C in width. The FP analysis allowed us to assign α' mode to reversible and isochronal phase transitions in the solid state. Such isochronal transitions have been already observed in liquid crystals [48], semi-crystalline ferroelectric polymers [49], collagen [50] and an elastin-derived peptide [51]. In previous studies on an elastin-derived peptide, such α' modes have been attributed to structural phase transitions consistent with the peculiar nanoscale crystalline ordering of this system. As shown for some model peptides, their self-assembly in the condensed state leads to macroscopic dipole moments explaining the enhancement of these dipolar properties (intense and sharp mode) [52]. These α' modes, sequence specific, are clearly connected to the different conformations (PPII helices, β sheets and β turns) of the studied peptides and can be the signature of ferroelectric materials, as already observed in synthetic ferroelectric polymers [49]. One of the aspects of biological systems is the intricate relationship between chemical and electrical functionalities. If the piezoelectricity of various biological tissues has been established since five decades [53, 54], only recent works demonstrated the ferroelectricity of soft biological tissues such as aortic walls [55], adding an important dimension to their biophysical properties and physiological functions. The ferroelectricity of elastin was also recently discovered, the polarization of this biomacromolecule being intrinsic at the monomer level [56]. Moreover, Heredia et al. [57] reported a robust and persistent nanoscale ferroelectricity of glycine in the piezoelectric γ phase and demonstrated that the ferroelectric behavior could persist at a single molecular level. This peculiar property of the simplest amino acid opens up interesting properties regarding the role of glycine in the self-assembly of peptides and protein formation.

In the [50; 100 °C] zone, a large relaxation peak (α) is evidenced for the three peptides. In contrast to the sharp α' modes, the α relaxation mode located from 81 °C for $(VGGLG)_3$ to 91 °C for $(VGGVG)_3$ extends over a wide temperature range, which is assigned to a large distribution

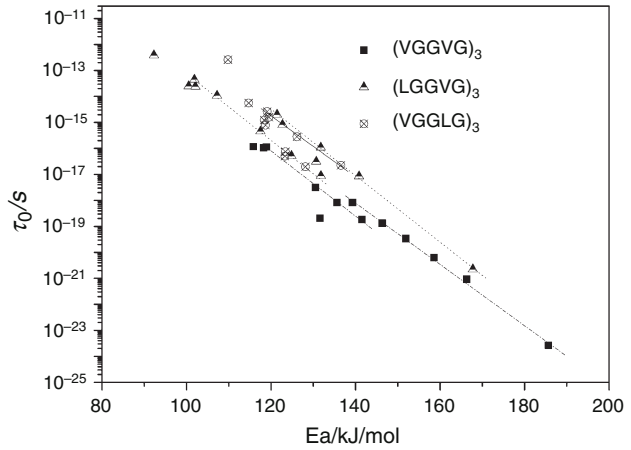

Fig. 11 Compensation diagram of the different elementary processes of the α mode of the pentadecapeptides from TSC/FP procedure

Table 1 Compensation parameters (T_c, τ_c) of the α mode for the pentadecapeptides

Sample	T_p range/ °C	T_{c1}/ °C	τ_{c1}/ s	T_p range/ °C	T_{c2}/ °C	τ_{c2}/s
$(VGGVG)_3$	60–75	148.2	0.06	80–105	170	0.024
$(LGGVG)_3$	55–75	142.5	0.3	90–105	132	10.6
$(VGGLG)_3$				90–100	173	0.204

of relaxing dipoles. The fine structure analysis of this relaxation mode was achieved through the TSC/FP method in the [60; 110 °C] for the three peptides. In this procedure, each isolated spectrum is well approximated by a single relaxation time, allowing Bucci–Fieschi's analysis [58]. The FP method allowed us to access the distribution of elementary relaxation times τ_i involved in the α mode. By plotting the variation of $\tau_i(T)$ versus temperature, we noted that all the extracted relaxation times were well fitted by an Arrhenius' law:

$$\tau_i(T) = \tau_{0i} \exp(E_{ai}/RT) \quad (1)$$

We reported in Fig. 11 the variation in the pre-exponential factor versus the activation energy for all the isolated relaxation times.

As previously described [38], the high values of the apparent activation energies combined with the very low values of the pre-exponential factor are indicative of cooperative processes. This fact is corroborated by the linear relationship that connects activation energy and logarithm of pre-exponential factor which corresponds to a compensation phenomenon:

$$\tau_{0a} = \tau_c \exp(-\Delta H/RT_c) \quad (2)$$

where T_c and τ_c correspond to the compensation temperature and the compensation time, respectively, and can be used as fingerprint of the dynamics.

As the temperature increases, the activation energy increases as well as the entropy activation that can be derived from the pre-exponential factor by

$$\tau_0 = h(kT)^{-1} \exp(-\Delta S/R) \quad (3)$$

The relaxation processes become complex, involving cooperative motions of neighboring segments. Observed in numerous polymers, proteins and polypeptides [32, 59], this behavior reflects the molecular mobility of dipolar species on some tens of nanometers and is attributed to the dielectric manifestation of the glass transition [29]. The maximum activation energy ΔH allows us to estimate the propagation length of the dipolar motions in the glassy state. As reported in Table 1 $(VGGVG)_3$ and $(LGGVG)_3$ are characterized by two compensation phenomena in the [55; 75 °C] and [80; 105 °C] windows, respectively, in contrast to $(VGGLG)_3$ which possesses a single compensation phenomenon in the high-temperature zone, reflecting a very distinct chain dynamics in this case. Moreover, the important decrease in the maximum activation energy for $(VGGLG)_3$ indicates the drastic restriction of the motion propagation length.

All these differences in the delocalized chain dynamics of the three peptides should be connected to the different conformations evidenced by FTIR in the solid state in the previous study [8]. The dominant unordered component of $(VGGLG)_3$ and the PPII extended structures leads to a softer system, as indicated by the shift toward low temperature of the α mode. The large amount of β sheets and β turns in $(VGGVG)_3$ and, in a lesser extent, in $(LGGVG)_3$ leads to stiffer systems as indicated by the high location of the α mode. This large amount of β sheets and β turns, with hydrogen bonds perpendicular to the chains, is also responsible for the propagation of delocalized motions over a larger scale than what offered by unordered and PPII conformations.

Conclusions

DSC and TSC studies on three pentadecapeptides, mimicking the main repetitive sequences of elastin, performed in identical conditions have clearly evidenced the strong effect of the sequence nature and order.

In solution, the evolution of surrounding water is a fine probe of the specific and multiple self-assembly processes of elastin-like peptides and can constitute the missing link with structural analysis.

In the solid state, the specific hydration behavior is brought to the fore and the distinct molecular mobilities at the nanoscopic and mesoscopic ranges help the knowledge of the different organization levels in the pre-fibrillar state. For the first time, it can be argued that the ferroelectricity of such elastin-like peptides certainly plays a key role in the self-assembly process of this protein.

References

1. Luan CH, Harris RD, Prasad KU, Urry DW. Differential scanning calorimetry studies of the inverse temperature transition of the polypentapeptide of elastin and its analogues. Biopolymers. 1990;29:1699–706.
2. Zhao B, Li NK, Yingling YG, Hall CK. LCST behavior is manifested in a single molecule: elastin-like polypeptide (VPGVG)n. Biomacromolecules. 2016;17:111–8.
3. Reguera J, Urry DW, Parker TM, McPherson DT, Rodríguez-Cabello JC. Effect of NaCl on the exothermic and endothermic components of the inverse temperature transition of a model elastin-like polymer. Biomacromolecules. 2007;8:354–8.
4. Ribeiro A, Arias FJ, Reguera J, Alonso M, Rodríguez-Cabello JC. Influence of the amino-acid sequence on the inverse temperature transition of elastin-like polymers. Biophys J. 2009;97:312–20.
5. Urry DW, Urry KD, Szaflarski W, Nowicki M. Elastic-contractile model proteins: physical chemistry, protein function and drug design and delivery. Adv Drug Deliv Rev. 2010;62:1404–55.
6. Kurzbach D, Hassouneh W, McDaniel JR, Jaumann EA, Chilkoti A, Hinderberger D. Hydration layer coupling and cooperativity in phase behavior of stimulus responsive peptide polymers. J Am Chem Soc. 2013;135:11299–308.
7. Meyer DE, Chilkoti A. Quantification of the effects of chain length and concentration on the thermal behavior of elastin-like polypeptides. Biomacromolecules. 2004;5:846–51.
8. Bochicchio B, Pepe A, Crudele M, Belloy N, Baud S, Dauchez M. Tuning self-assembly in elastin-derivd peptides. Soft Matter R Soc Chem. 2015;11:3385–95.
9. Rodrıguez-Cabello JC, Alonso M, Perez T, Herguedas MM. Calorimetry study of the hydrophobic hydration of the poly (VPGVG), from deficiency. Biopolymers. 2000;54:282–8.
10. Urry DW, Trapane TL, Prasad KU. Phase-structure transitions of the elastin polypentapeptide-water system within the framework of composition-temperature studies. Biopolymers. 1985;24:2345–56.
11. Bochicchio B, Floquet N, Pepe A, Alix AJP, Tamburro AM. Dissection of human tropoelastin: solution structure, dynamics and self-assembly of the exon 5 peptide. Chem Eur J. 2004;10:3166–76.
12. Pepe A, Armenante MR, Bochicchio B, Tamburro AM. Formation of nanostructures by self-assembly of an elastin peptide. Soft Matter. 2009;5:104–13.
13. Tamburro AM, Lorusso M, Ibris N, Pepe A, Bochicchio B. Investigating by circular dichroism some amyloidogenic elastin-derived polypeptides. Chirality. 2010;22:E56–66.
14. Tamburro AM, Bochicchio B, Pepe A. The dissection of human tropoelastin: from the molecular structure to the self-assembly to the elasticity mechanism. Pathol Biol. 2005;53:383–9.
15. Rauscher S, Baud S, Miao M, Keeley FW, Pomès R. Proline and glycine control protein self-organization into elastomeric or amyloid fibrils. Structure (London, England: 1993). 2006;14:1667–76.
16. Cirulis JT, Keeley FW, James DF. Viscoelastic properties and gelation of an elastin-like polypeptide. J Rheol. 2009;53:1215–28.
17. Miao M, Bellingham CM, Stahl RJ, Sitarz EE, Lane CJ, Keeley FW. Sequence and structure determinants for the self-aggregation of recombinant polypeptides modeled after human elastin. J Biol Chem. 2003;278:48553–62.
18. Muiznieks LD, Reichheld SE, Sitarz EE, Miao M, Keeley FW. Proline-poor hydrophobic domains modulate the assembly and material properties of polymeric elastin. Biopolymers. 2015;103:563–73.
19. Le DHT, Hanamura R, Pham DH, Kato M, Tirrell DA, Okubo T, Sugawara-Narutaki A. Self-assembly of elastin–mimetic double hydrophobic polypeptides. Biomacromolecules. 2013;14:1028–34.
20. Salvi AM, Moscarelli P, Satriano G, Bochicchio B, Castle JE. Influence of amino acid specificities on the molecular and supramolecular organization of glycine-rich elastin-like polypeptides in water. Biopolymers. 2011;95:702–21.
21. Salvi AM, Moscarelli P, Bochicchio B, Lanza G, Castle JE. Combined effects of solvation and aggregation propensity on the final supramolecular structures adopted by hydrophobic, glycine-rich, elastin-like polypeptides. Biopolymers. 2013;99:292–313.
22. Tamburro AM, Bochicchio B, Pepe A. Dissection of human tropoelastin: exon-by-exon chemical synthesis and related. Biochemistry. 2003;42:13347–62.
23. Moscarelli P, Boraldi F, Bochicchio B, Pepe A, Salvi AM, Quaglino D. Structural characterization and biological properties of the amyloidogenic elastin-like peptide $(VGGVG)_3$. Matrix Biol. 2014;36:15–27.
24. Flamia R, Zhdan PA, Martino M, Castle JE, Tamburro AM. AFM study of the elastin-like biopolymer poly(ValGlyGlyValGly). Biomacromolecules. 2004;5:1511–8.
25. Ostrowska-Ligęza E, Górska A, Wirkowska M, Koczoń P. An assessment of various powdered baby formulas by conventional methods (DSC) or FT-IR spectroscopy. J Therm Anal Calorim. 2012;110:465–71.
26. Briere LAK, Brandt JM, Medley JB. Measurement of protein denaturation in human synovial fluid and its analogs using differential scanning calorimetry. J Therm Anal Calorim. 2010;102:99–106.
27. Suh Y, Kim BJ, Tam KC, Aucoin MG. Detection and characterization of hemoglobin dissociation and aggregation using microcalorimetry. J Therm Anal Calorim. 2013;115:2159–69.
28. Tiné MR, Alderighi M, Duce C, Ghezzi L, Solaro R. Effect of temperature on self-assembly of an ionic tetrapeptide. J Therm Anal Calorim. 2010;103:75–80.
29. Megret C, Guantieri V, Lamure A, Pieraggi MT, Lacabanne C, Tamburro AM. Phase transitions and chain dynamics, in the solid state, of a pentapeptide sequence of elastins. Int J Biol Macromol. 1992;14:45–9.
30. Rodriguez-Cabello JC, Alonso M, Diez MI, Caballero MI, Herguedas MM. Structural investigation of the poly(pentapeptide) of elastin, poly(GVGVP), in the solid state. Macromol Chem Phys. 1999;200:1831–8.
31. Dandurand J, Samouillan V, Lacabanne C, Pepe A, Bochicchio B. Water structure and elastin-like peptide aggregation. J Therm Anal Calorim. 2015;120:416–26.
32. Teyssedre G, Mezghani S, Bernes A, Lacabanne C. Thermally stimulated currents of polymers. In: Runt J, Fitzgerald J, editors. Dielectric spectroscopy of polymeric materials. Fundamental and applications. Washington: American Chemical Society; 1997. p. 227.
33. Samouillan V, Lamure A, Maurel E, Dandurand J, Lacabanne C, Ballarin F, et al. Characterisation of elastin and collagen in aortic bioprostheses. Med Biol Eng Comput. 2000;38:226–31.

34. Samouillan V, Tintar D, Lacabanne C. Hydrated elastin: dynamics of water and protein followed by dielectric spectroscopies. Chem Phys. 2011;385:19–26.
35. Samouillan V, André C, Dandurand J, Lacabanne C. Effect of water on the molecular mobility of elastin. Biomacromolecules. 2004;5:958–64.
36. Megret C, Guantieri V, Lamure A, Pieraggi MT, Lacabanne C. Solid-state studies on synthetic fragments and analogues of elastin. Int J Biol Macromol. 1993;15:305–12.
37. Tintar D, Samouillan V, Dandurand J, Lacabanne C, Pepe A, Bochicchio B, Tamburro AM. Human tropoelastin sequence: dynamics of polypeptide coded by exon 6 in solution. Biopolymers. 2009;91:943–52.
38. Samouillan V, Dandurand J, Lacabanne C. Dielectric spectroscopy and thermally stimulated current analysis of biopolymer systems. In: Sabu T, Durand D, Chassenieux C, Jyotishkumar P, editors. Handbook of biopolymer-based materials. 1st ed. Weinheim: Wiley-VCH Verlag GmbH & Co KGaA; 2013. p. 371.
39. Teeter MM. Water structure of a hydrophobic protein at atomic resolution: pentagon rings of water molecules in crystals of crambin. Proc Natl Acad Sci USA. 1984;81:6014–8.
40. Nilsson MR. Techniques to study amyloid fibril formation in vitro. Methods. 2004;34:151–60.
41. Yamaoka T, Tamura T, Seto Y, Tada T, Kunugi S, Tirrell DA. Mechanism for the phase transition of a genetically engineered elastin model peptide $(VPGIG)_{40}$ in aqueous solution. Biomacromolecules. 2003;4:1680–5.
42. Castle JE, Salvi M, Ibris N, Moscarelli P, Bochicchio B, Pepe A. Characterisation of helical structure in AFM micrographs of a trimer of the peptide sequence (ValGlyGlyValGly). Surf Interface Anal. 2014;. doi:10.1002/sia.5446.
43. Nakamura K, Hatakeyama T, Hatakeyama H. Studies on bound water of cellulose by differential scanning calorimetry. Text Res J. 1981;51:607–13.
44. Clausse D, Wardhono EY, Lanoiselle JL. Formation and determination of the amount of ice formed in water dispersed in various materials. Colloids Surf A Physicochem Eng Asp. 2014;460:519–26.
45. Butler AV. The energy and entropy of hydration of organic compounds. Trans Faraday Soc. 1937;33:229–38.
46. Swenson J, Jansson H, Hedström J, Bergman R. Properties of hydration water and its role in protein dynamics. J Phys Condens Matter. 2007;19:205109.
47. Mijović J, Bian Y, Gross RA, Chen B. Dynamics of proteins in hydrated state and in solution as studied by dielectric relaxation spectroscopy. Macromolecules. 2005;38:10812–9.
48. Kripotou S, Georgopoulos D, Kyritsis A, Pissis P. Molecular mobility in the molecular liquid crystal 5CB. Mol Cryst Liq Cryst. 2015;623:407–23.
49. Teyssedre G, Bernes A, Lacabanne C. DSC and TSC study of a VDF/TrFE copolymer. Thermochim Acta. 1993;226:65–75.
50. Samouillan V, Lamure A, Lacabanne C. Dielectric relaxations of collagen and elastin in the dehydrated state. Chem Phys. 2000;255:259–71.
51. Samouillan V, Dandurand J, Causse N, Lacabanne C, Bochicchio B, Pepe A. Influence of the architecture on the molecular mobility of synthetic fragments inspired from human tropoelastin. IEEE Trans Dielectr Electr Insul. 2015;22:1427–33.
52. Bystrov VS, Bdikin I, Heredia A, Pullar RC, Mishina ED, Sigov AS, Kholkin AL. Piezoelectricity and ferroelectricity in biomaterials: from proteins to self-assembled peptide nanotubes. In: Giofani G, Menciassi A, editors. Piezoelectric Nanomaterials for Biomedical Applications. Berlin: Springer; 2012. p. 187–212.
53. Braden M, Barstow A, Brider I, Ritter B. Electrical and piezoelectrical properties of dental hard tissues. Nature. 1966;212:1565–6.
54. Fukada E, Ueda H, Rinaldi R. Piezoelectric and related properties of hydrated collagen. Biophys J. 1976;16:911–8.
55. Liu Y, Cai H-L, Zelisko M, Wang Y, Sun J, Yan F, Ma F, Wang P, Chen QN, Zheng H, Meng X, Sharma P, Zhang Y, Li J. Ferroelectric switching of elastin. Proc Natl Acad Sci USA. 2014;111:E2780–6.
56. Liu Y, Zhang Y, Chow MJ, Chen QN, Li J. Biological ferroelectricity uncovered in aortic walls by piezoresponse force microscopy. Phys Rev Lett. 2012;108:1–5.
57. Heredia A, Meunier V, Bdikin IK, Gracio J, Balke N, Jesse S, Tselev A, Agarwal PK, Sumpter BG, Kalinin SV, Kholkin AL. Nanoscale ferroelectricity in crystalline γ-glycine. Adv Funct Mater. 2012;22:2996–3003.
58. Bucci C, Fieschi R, Guidi G. Ionic thermocurrents in dielectrics. Phys Rev. 1966;148:816–23.
59. Samouillan V, Dandurand J, Lacabanne C, Hornebeck W. Molecular mobility of elastin: effect of molecular architecture. Biomacromolecules. 2002;3:531–7.